



Risk Assessment and Mechanism of Water Inrush in Water-rich Deep-buried Karst Tunnel

Xin Zhang^{1,2}, Mingtang Lei¹, Shaoqing Wang³, Xiaotian Zhang⁴, Hai Chen⁵,

Xiaozhen Jiang^{1,*}

5 ¹Institute of Karst Geology, Chinese Academy of Geological Sciences, Guilin 541004, China

²China University of Geosciences, Beijing 100083, China

³Zhongzi Huake Transportation Construction Technology Co., Ltd. Beijing 100039, China

⁴CCCC Infrastructure Maintenance Group Co., Ltd. Beijing 100010, China

⁵Hunan Provincial Communications Planning, Survey & Design Institute Co., Ltd.

10 Changsha 410008, China

*Corresponding email: m18813050910@163.com (Xiaozhen Jiang)

Abstract

Water inrush disaster is the main geological disaster of water-rich and deep-buried karst tunnel, which is extremely harmful and threatens tunnel construction and construction safety. When building tunnels
15 in water-rich and deep-buried karst areas, it has become a major challenge to evaluate the risk and study the mechanism of water inrush from tunnels. In order to solve this problem, this paper takes Nahecun water-rich deep-buried karst tunnel of Tian'e through Fengshan to Bama to Expressway as the research object, analyzes the hydrogeological characteristics of karst area through geological investigation, grasps the characteristics of groundwater occurrence and migration, finds out the main disaster-causing
20 factors and influencing factors of water inrush disaster in karst tunnel, reasonably selects the influencing factors of water inrush and their weights to construct a combined weighting -TOPSIS method tunnel water inrush risk assessment system, verifies the evaluation system through field excavation experiments, and analyzes the water inrush mechanism of karst tunnel by using finite element analysis software. The research results show that the main influencing factors of water inrush in karst tunnel
25 include stratum, geological structure, topography, hydrogeological conditions and other factors. The evaluation weight of each index is obtained by using analytic hierarchy process and entropy weight method, and the distance and relative proximity between the typical tunnel section and the ideal solution



are obtained according to the combined weight -TOPSIS method, so as to evaluate the water inrush risk of Nahecun tunnel section. Based on the equivalent continuum model and Hoek-Brown yield criterion, a three-dimensional simulation model of Nahecun tunnel is established, and the pore water pressure of initial stress-seepage coupling and secondary stress-seepage coupling after excavation is carried out. It is concluded that the pore water pressure near the two sides of the cave is higher than that above, and the area with higher pore water pressure near the cave on the left is concentrated around the cave, while the pore water pressure on the right side is dispersed. The pore water pressure around the initial coupling cave is obviously higher than that around the secondary coupling cave, and the maximum pore water pressure on the left side of the cave is greater than that on the right side of the cave. The research results provide theoretical data support for water inrush risk assessment and water inrush mechanism research of deep-buried karst tunnel with rich water.

Key words

karst tunnel; Water inrush risk; Water inrush mechanism; Combination empowerment -TOPSIS

1 Introduction

With the rapid development of infrastructure projects in China and the continuous improvement of construction technology, there are more and more tunnel projects in karst areas, but water inrush often occurs in karst tunnel construction, which brings great problems to the construction (Liu et al., 2019). The water inrush disaster of karst tunnel is mainly in tunnel construction. Because the underground aquifer is destroyed, the water resistance of rock stratum is weakened, and groundwater breaks through the water-resisting layer and flows into the tunnel under the head pressure. At present, due to the limited space of tunnel engineering, once a water inrush accident occurs, it is difficult to evacuate personnel and equipment, causing huge losses to life and property. Water-rich and deep-buried karst tunnel has many hydrogeological units exposed by the tunnel, abundant water source, large water inflow and high head pressure. When the tunnel excavation changes the migration and discharge of groundwater, it is very easy to have an instantaneous water inrush of more than 10,000 tons, resulting in the complete damage of the tunnel being excavated, resulting in the disaster of machine destruction and personal injury. Therefore, when building tunnels in high-pressure and water-rich areas, it is of great practical



55 significance to carry out the risk assessment and mechanism research of water inrush in tunnels.(Shan et al., 2022;He et al., 2023;Yang et al., 2019;Huang et al., 2022; Jiang et al., 2019).

In order to investigate the influence of variations in groundwater gas pressure on karst collapse within the fissure system of karst conduits.Lei mingtang and Jiang xiaozhen successively successively conducted research on karst collapse phenomena within multiple cities such as Tangshan, Yulin, and
60 Xiangtan. Through the implementation of techniques involving karst water extraction and the utilization of sensors to capture the continuous variations in groundwater pressure within karst fissure or conduit systems, alterations were induced in the hydraulic (gas) pressure of the karst conduit fissure system. This alteration intensified the subsurface groundwater seepage process within the Quaternary strata. When hydraulic gradients attained the threshold for initiating permeation failure within the strata,
65 structural failure occurred, consequently giving rise to collapses. It is notably emphasized that the fluctuation in karst groundwater and gas pressures stands as the principal inducing factor responsible for the occurrence of karst collapses (Tang et al., 2023). Some research results have been made on the risk assessment and water inrush mechanism of tunnel. Sun et al. (2022) put forward a rapid evaluation method of karst tunnel safety. By analyzing the influencing factors of water inrush disaster in karst
70 tunnel, the rapid evaluation method of water inrush and mud outburst prevention in karst tunnel was established by selecting factors such as hydrodynamic conditions, bad geology, outburst prevention thickness and surrounding rock characteristics, and the influencing factors were divided into main, secondary and correction factors. By evaluating the water inrush project of Chongqing-Yichang railway large tunnel, it was concluded that this evaluation method solved the deficiency of traditional water
75 inrush risk evaluation without considering the surrounding rock characteristics and thickness, and it was also verified. Jiang et al. (2022) put forward the comprehensive weighting -TOPSIS method for the risk assessment of tunnel water inrush. By analyzing the existing methods of water inrush risk assessment, the evaluation results are vague and the evaluation indicators are not fully quantified, and it is proposed to combine TOPSIS method, AHP method and coefficient of variation method, and comprehensively
80 weight the subjective and objective factors to construct four water inrush risk grade samples. The risk assessment system of tunnel water inrush based on TOPSIS method is established, and it is applied to Xiangyun tunnel and Beitianshan tunnel of railway, and the risk assessment of tunnel water inrush is



carried out in eight sections. It is concluded that the comprehensive weighting -TOPSIS method is more accurate (Wang et al., 2021; Wang et al., 2020). Liu et al. (2023) studied the mechanism of sudden flood
85 of filling karst pipeline in highway tunnel, established three kinds of mechanical instability models by analyzing the water inrush structure of geological defect karst, and obtained their instability criteria. Based on the karst water inrush event in DEOCA tunnel, the micro-and macro-evolution process of sudden flood of karst pipeline was simulated by using the real karst rupture process analysis programs RFPA and Flac3D. It is concluded that the safety factor of the filling body of karst pipeline has reached
90 0.46, and the filling body has already experienced sliding instability and karst water inrush. The numerical simulation results are consistent with the actual water inrush in the field, which well reflects the evolution mechanism of the whole process of water inrush in karst pipeline . Liu et al. (2021) put forward a water inrush risk assessment system based on comprehensive weighting method. Considering the complex geological conditions of underground engineering, based on the theory of attribute
95 mathematics, an attribute interval assessment theory and an attribute identification analysis method for quantitative evaluation were established. By selecting seven typical influencing factors of karst water inrush disaster, an index system and an evaluation model for water inrush risk were constructed, and the weight of water inrush risk indicators was analyzed by comprehensive weighting method. The rationality and feasibility of the index system and evaluation model were verified by examples. Li et al.
100 (2023) studied the mechanism of tunnel water inrush, taking the deep-buried karst tunnel as the research object, analyzed the main forms of underground karst development, and analyzed the interaction between surface water, groundwater and rocks in the tunnel. It was expounded that the rock fracture caused by fracture mechanics destroyed the surrounding rock of the tunnel, formed a water inrush channel, and caused tunnel water inrush, and analyzed the water inrush mechanism.

105 When building tunnels in water-rich and deep-buried karst areas, it has become a major challenge to evaluate the risk and study the mechanism of water inrush from tunnels. This paper takes Nahecun water-rich deep-buried karst tunnel of Tian'e through Fengshan to Bama Expressway as the research object, analyzes the hydrogeological characteristics of karst area through geological investigation, grasps the characteristics of groundwater occurrence and migration, finds out the main disaster-causing
110 factors and influencing factors of water inrush disaster in karst tunnel, reasonably selects the influencing



factors of water inrush and their weights to construct a combined weighting -TOPSIS method tunnel water inrush risk assessment system, verifies the evaluation system through field excavation experiments, and analyzes the water inrush mechanism of karst tunnel by using finite element analysis software, which provides the water inrush risk assessment and water inrush mechanism research for
115 water-rich deep-buried karst tunnel.

2 Research Methods

2.1 Engineering geological characteristics of the study area

Tian'e through Fengshan to Bama Expressway is located in Hechi City, Guangxi Zhuang Autonomous Region, the route is generally north-south direction, the total length of 105Km. the whole line is a
120 mountainous and hilly area, by the tectonic effect of significant impacts, stripping, erosion, erosion, the entire line of terrain is high and steep, terrain cutting serious, peaks between the mountains, more steep walls, depressions, dark river. The average annual rainfall in the area is generally between 1500 and 2000mm, with more than 2500mm in many places and more than 1000mm in the least, and April to September is the rainy season, with its precipitation accounting for 70 to 85% of the annual
125 precipitation, which is prone to floods, so the tunnel needs to overcome many key waterproofing technical problems in the process of design and construction.

The tunnel is located in the southwest of Nahuo Village, Tian'e County, Hechi City, and is the controlling tunnel project of Tianba Road, with a total length of 2.77Km and a maximum depth of about 551.68 m. The tunnel site area is located in a high mountainous area, with a steeper hill, belonging to
130 the karst rocky peaks and puddles geomorphology. According to the physical exploration, drilling and geological survey, the strata in the tunnel area are mainly the residual slope accumulation layer of the Quaternary System, the Maokou Formation of the Permian System, the Qixia Formation of the Lower Permian System and the Upper Carboniferous System, and the exposed lithology is mainly medium-weathered and strongly weathered greywacke. Surface karst morphology is characterized mainly by
135 dissolution scars, dissolution gaps, dissolution grooves, dissolution grooves and dissolution holes, and funnels, dissolution depressions (dissolution valleys), dissolution caves, and negative topographic features can be seen in the axial area of the tunnel, and the depth of karst development is relatively shallow, which belongs to the area of strong development of karst. The tunnel passes through the



Yunbang backslope, from the two wings to the core, the backslope is 40Km long, the core and the wing
140 of the lithology is dominated by tuff, and the rock body is more broken. Tunnel entrance section, cave
section, exit section mainly develops six groups of joints and fissures, the joint surface is rough, shallow
joint surface dissolution is strong, the opening is obvious, filled with clay. During the construction
process, the rock and soil bodies are subjected to the erosion of karst water, which greatly reduces the
strength of the surrounding rock structure, resulting in sudden water and mud accidents (Li et al., 2023).
145 The entrance and exit section of the tunnel in Nakhchon village has developed gullies and valleys,
which are the gathering area of surface water, and the water flow is controlled by the atmospheric
rainfall, and the surface converges and then automatically runs off to the northwest direction, and
eventually converges into surface streams and gullies discharging to the Hongshui River near the tunnel.
The tunnel body is located below the depression, so it is greatly influenced by the infiltration and
150 recharge of surface water. According to the survey data, the groundwater in the tunnel site area is
dominated by the pore water of the fourth system and carbonate fissure karst water, and the runoff mode
is dominated by the fissure - pipeline type, with both pipeline - fissure type and fissure type, and the
groundwater runoff is in the karst pipeline, with the runoff pathway being long, and the flow rate,
hydraulic gradient and dynamics changing greatly, and it is discharged by the The underground river is
155 concentrated to the northwest of the discharge datum of the Hongshui River tributary discharge. Tunnel
K7+720 at the development of an underground river, the surface depression and underground river pipe
often form vertical slit dissolution channel, is the surface water through the water dissipation hole
infiltration recharge to the groundwater of the main water conduit, when the tunnel in the tunnel through
the slit vertical dissolution channel, due to the rainy season rainfall injection of large amounts of water,
160 the construction of tunnels will produce a greater threat (Dai et al., 2019).

2.2 tunnel water inrush risk assessment index

Water inrush in karst tunnel is caused by the karst water-bearing structure or changing the mechanical
state of surrounding rock, breaking the original equilibrium state and causing water inrush during tunnel
excavation. The main influencing factors of water inrush in karst tunnels are stratum, geological
165 structure, topography, hydrogeology and so on (Han et al., 2023). By selecting the influencing factors



of karst tunnel water inrush and comprehensively analyzing the occurrence of karst tunnel water inrush disaster, the risk assessment system of karst tunnel water inrush is constructed.

Based on the geological exploration of Nahecun tunnel, this paper establishes an evaluation index system of water inrush risk in karst tunnel, which mainly includes five evaluation indexes: stratum factor A, geological structure factor B, landform factor C, hydrogeological condition factor D and other factors E (Zhang et al., 2019). Table 1 gives the risk assessment index system of water inrush in karst tunnels.

Table 1 Risk Assessment Index of Water Inrush in Karst Tunnel

evaluating indicator	Main parameter
Stratigraphic factor a	Lithology and rock occurrence
Geological structural factor b	Faults and folds
Topographic factor c	Negative terrain area and terrain slope
Hydrogeological condition factor d	Difference between underground water level and tunnel elevation, water pressure of karst cave
Other factors e	In-situ stress and cave diameter

Stratigraphic factors mainly consider lithology and rock occurrence. Lithology is mainly quantitatively analyzed through the soluble rock content of rock strata. When the proportion of soluble rocks is higher, the karst is more developed and the karst space is larger. Generally, the content of CaCO₃ is used as the division standard (Zhang et al., 2019). Rock attitude, that is, rock dip angle, in which the most favorable rock dip angle for karst development is 25 ~ 65. Table 2 gives the classification table of formation factors.

Table 2 Classification Table of Stratigraphic Factors

Grading	rock character	Rock occurrence
	CaCO ₃ content (%)	Dip angle of strata (degree)
I	70-100	45-60
II	50-70	30-45



III	30-50	15-30
IV	0-30	0-15

Geological structure mainly considers two evaluation indexes: fault and fold(Luo et al., 2023). Fault evaluation is mainly based on fault width, and fold evaluation is mainly graded according to the size of fold development, and expert scoring system is adopted, with 0 ~ 100 as quantitative scoring. Table 3 gives the geological structure classification table.

Table 3 Geological Structure Classification Table

Grading	fault	fold
	Fault width (m)	Score value of wrinkle development degree
I	>10	70-100 syncline structure
II	5-10	50-70 anticline with developed fractures
III	2-5	30-50 anticline with well-developed fractures
IV	0-2	0-30 has small folds or no folds.

Topography mainly considers negative topographic area and topographic slope(Dong et al., 2023). With the increase of negative terrain area, it shows that the terrain has strong water accumulation and karst development; With the gradual slope of the terrain, the slower the water flow speed, and the longer the water stays in the rock stratum, the water easily permeates and the rock stratum is more likely to form karst. Table 4 gives the classification table of topography and geomorphology.

Table 4 Classification Table of Topography and Geomorphology

Grading	Negative terrain area ratio (%)	Surface slope (degree)
I	80-100	0-10
II	50-80	10-25



III	20-50	25-45
IV	0-20	>45

Hydrogeological factors mainly consider the difference between groundwater level and tunnel elevation and the water pressure of karst caves(Fu et al., 2021). In view of the elevation difference between groundwater level and tunnel buried depth, it has a great influence on tunnel construction water inrush. Groundwater is the key element of karst tunnel water inrush, and the local groundwater level is above the tunnel, which is the most harmful to tunnel water inrush. At the same time, the water pressure in the karst cave also directly affects the water inrush in the tunnel. When the water pressure in the karst cave is high, the water flow in the tunnel where the water inrush occurs is very large, so the water inflow is also large and the water inrush level in the tunnel is also high. Table 5 gives the hydrogeological classification table.

Table 5 Hydrogeological Classification Table

Grading	Water level difference (m)	Karst cave water pressure (MPa)
I	>60	15-20
II	30-60	10-15
III	10-30	5-10
IV	≤10	0-5

Other factors mainly include in-situ stress and cave diameter(Jana et al., 2021). In-situ stress increases with the increase of rock depth. The deeper the tunnel is buried, the greater the in-situ stress is, and the surrounding rock is more prone to deformation and failure, resulting in water inrush accidents. At the same time, the larger the karst cave is in the karst development area, the more abundant groundwater is in it. Once the large-diameter water-filled cave is drilled, the consequences of water inrush are very serious. Table 6 gives the ranking table of other factors.

Table 6 Other Factors Grading Table

Grading	Buried depth of tunnel (m)	Cave diameter (m)
---------	-------------------------------	-------------------



I	> 500	> 20 oversize
II	300-500	10-20 large
III	100-300	5-10 medium-sized
IV	0-100	0-5 small

3 Experimental Results

210 3.1 TOPSIS water inrush risk assessment based on combination weighting method

By using analytic hierarchy process (AHP), the strata, geological structure, topography, hydrogeological conditions and other factors are compared and analyzed, and a judgment matrix is established according to the importance of experts' evaluation indexes of water inrush. The maximum eigenvalue and corresponding eigenvector of the matrix are solved by using the eigenvector method and matlab software(Zhang et al., 2024). According to the calculation results of each evaluation index by analytic hierarchy process, the weight of water inrush evaluation index is obtained.

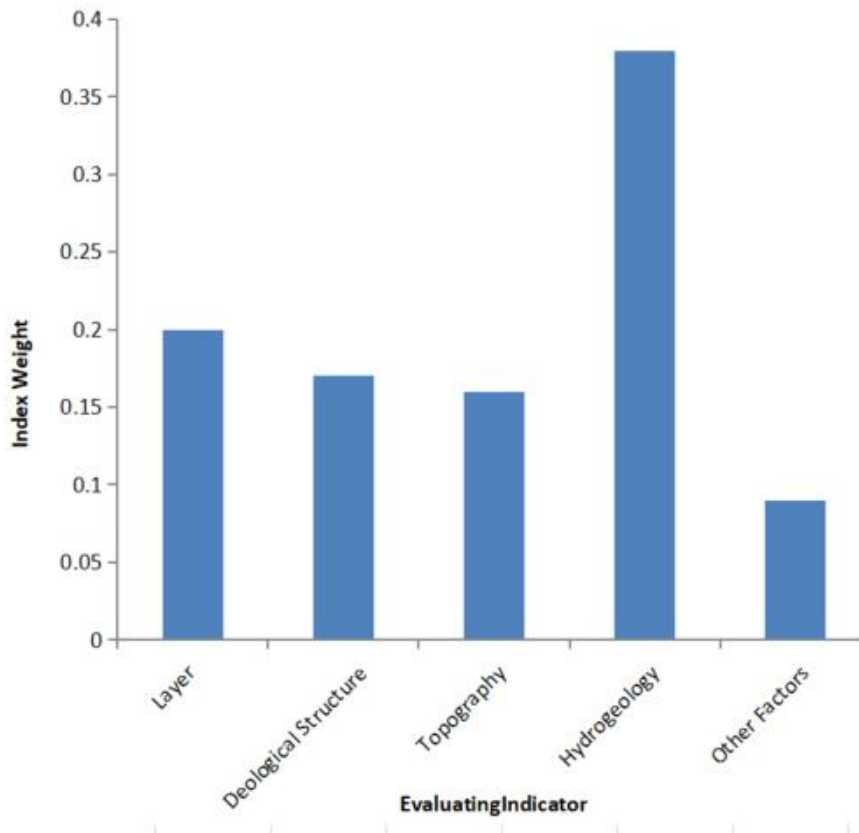




Figure 1 Weight of water inrush evaluation index based on analytic hierarchy process

Entropy weight method is an objective weighting method. The smaller the entropy of a result, the
220 greater the difference of its indicators, and the greater the role and weight in comprehensive evaluation
(Su et al., 2024;Xiao et al., 2024). By establishing the original data matrix of evaluation indexes and
evaluation objects, the proportion of each evaluation index is calculated, and the proportion matrix is
established based on the proportion data, and the index information entropy value and information
effect value of each index are calculated, thus the evaluation weight of each index is obtained. Figure 2
225 gives the weight of water inrush evaluation index based on entropy weight method.

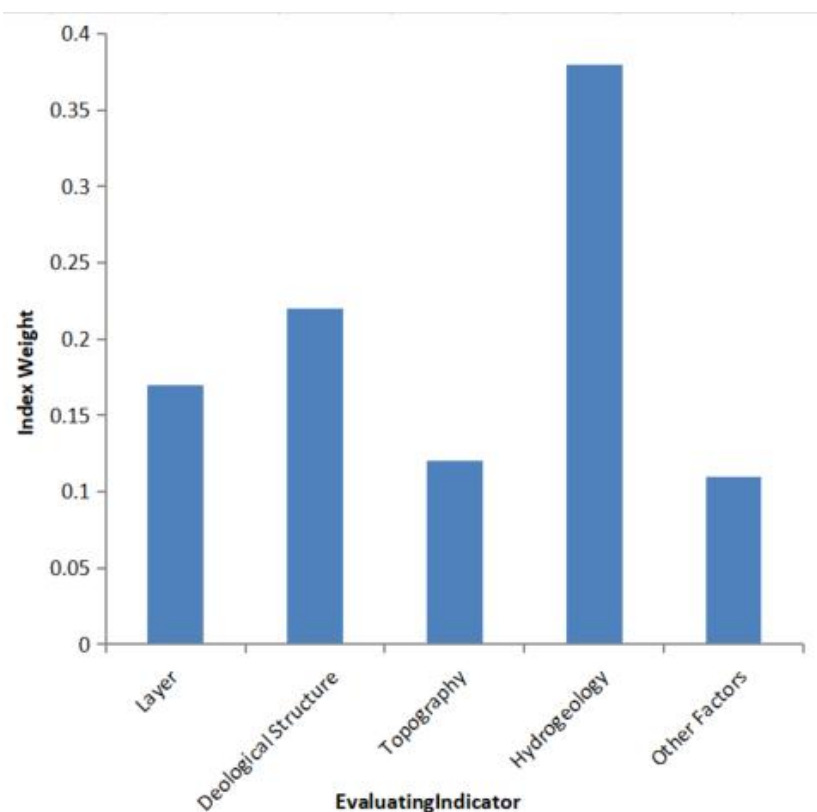


Figure 2 Weight of water inrush evaluation index based on entropy weight method

According to the weight vector of each water inrush evaluation index obtained by AHP and entropy
weight method, it is assumed that there are five evaluation indexes of water inrush evaluation index, and
230 their evaluation values constitute a decision matrix; The comprehensive weight is used to process each
index value, and the initial evaluation matrix is established with four samples of different grades.



Because there are some differences in the dimensions and orders of magnitude of each water inrush evaluation index, some evaluation index values are higher, while others are lower. In order to avoid the influence of different dimensional units among each water inrush evaluation index on the calculation results, each evaluation index is standardized, and the initial evaluation matrix is differentiated from the positive index and the negative index, and the initial matrix is initialized to obtain a standardized decision matrix, which is then combined with the initial weighted matrix to obtain a weighted standardized decision matrix. The distance from each water inrush level to the positive ideal solution and the distance from the negative ideal solution are obtained by solving, and then the relative proximity of each water inrush level is calculated according to the formula to form the corresponding judgment interval of each water inrush level. Fig. 3 shows the distance between each water inrush level and the ideal solution. Table 7 gives the close proximity values of each water inrush level.

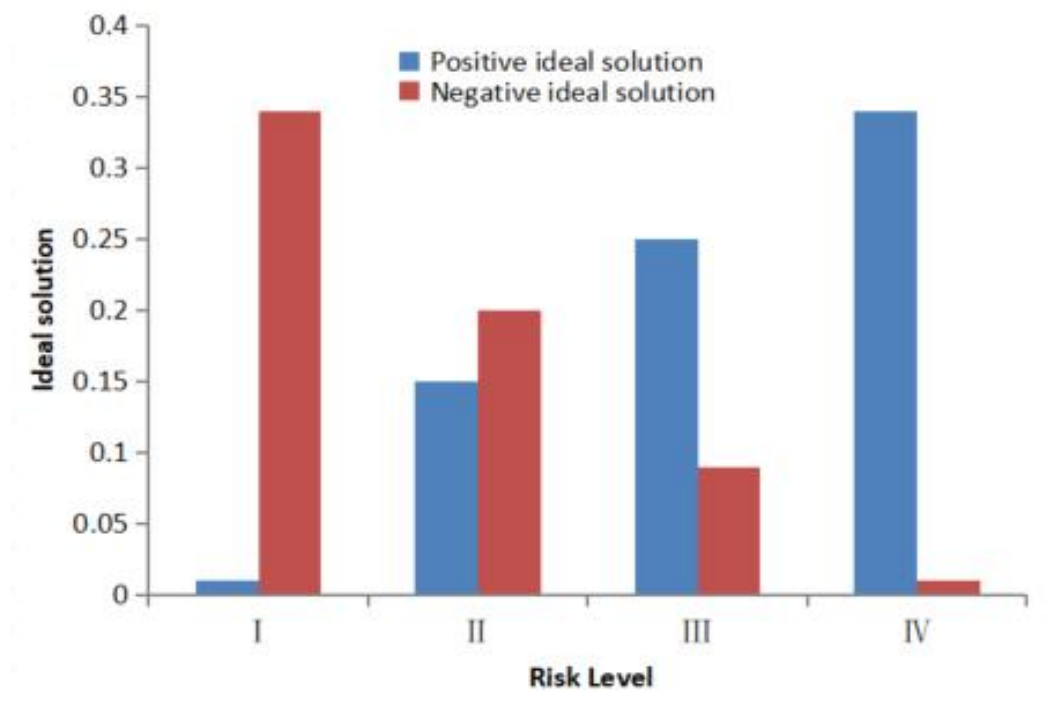


Figure 3 Distance between water inrush levels and ideal solution

245 **Table 7 Distance and approximate proximity between each water inrush level and ideal solution**

risk level	Relative closeness of
------------	-----------------------



positive ideal solution	
I	1
II	0.58-1
III	0.27-0.58
IV	0-0.27

According to the combined weighting -TOPSIS method, the water inrush risk of Nahecun tunnel section is evaluated, and the distance and relative proximity between the typical tunnel section and the ideal solution are obtained. Table 8 gives the evaluation results of water inrush risk in typical tunnel sections.

Table 8 Water inrush risk assessment results of typical tunnel sections

Typical tunnel section	Positive ideal solution	Negative ideal solution	Relative closeness of positive ideal solution	risk level
K6+250~K6+490	0.27	0.18	0.39	III
K7+750~K7+950	0.16	0.27	0.63	II
K8+660~K8+850	0.18	0.25	0.58	II
K9+240~K9+560	0.29	0.14	0.3224	III

250 3.2 Water inrush mechanism of karst tunnel

Based on the coupling theory of seepage field and stress field, the mechanism of water inrush in karst tunnel is studied through the fact that the maximum buried depth of Nahecun tunnel is 551 meters and it is in the state of high water abundance and high ground stress. In this paper, finite element analysis software is used to study the mechanism of water inrush in tunnel sections with risk grade II K7+750 ~
 255 K7+950.

K7+750 ~ K7+950 tunnel section, the stratum is Lower Permian Maokou Formation, the lithology is thick dark gray limestone, the tunnel rock is hard and complete, and the surrounding rock is Grade II surrounding rock. The landform is relatively flat, the surface slope exceeds 30, the strike of rock stratum is 80, and the dip angle of rock stratum is 45. The folds are well developed and belong to the axis of
 260 anticline. The groundwater is mainly karst fissure water and karst fissure water, which is extremely rich



in water, and the groundwater in some areas is confined. The tunnel is buried at a depth of 430 meters, and a cave with a diameter of 4 meters has been found. The distance between the cave and the tunnel is 5 meters, and the water pressure is about 10MPa. There is no fault around the tunnel section, and the surface where the tunnel section is located has negative topography, which is small in scale.

265 The equivalent continuum model is adopted, the surrounding rock is assumed to be isotropic elastic-plastic material, and Hoek-Brown yield criterion is adopted, ignoring all kinds of karst development around the actual karst cave, which is full of water and confined water. In the calculation process, the karst cave is simplified as a circular model. According to the design drawing of Nahecun tunnel, the tunnel section is determined to be horseshoe-shaped, with a width of 12m and a height of 9m, and a 3D

270 simulation model of Nahecun tunnel is established. In the model, the X direction is the tunnel width direction, the Y direction is the tunnel length direction, and the Z direction is the depth direction. A three-dimensional numerical model of 60m×60m×60m is established, and there is a water-filled cave with a diameter of 4m on the right side of the tunnel, and the center of the tunnel is the center of the model.

275 According to the geological exploration data and related design documents of Nahecun tunnel, and combined with the parameters of surrounding rock of relevant tunnels on site, the selection is made. The periphery and bottom of the model are set as impermeable boundaries, the initial condition is that the water pressure in the cave is 10MPa, and the tunnel wall and tunnel face are the water outlet boundaries; Horizontal constraints are set on the left and right sides of the tunnel model, the bottom is fully

280 constrained, and the top and the inside of the tunnel are free surfaces to constrain the displacement of the bottom boundary of the model; The initial stress in the model is calculated according to the self-weight stress of rock mass, and the lateral pressure coefficient is 1. According to the empirical formula of ground stress, the dead weight stress of K7+750 ~ K7+950 tunnel section is set to 30MPa, the lateral pressure coefficient is 1, and the horizontal stress is 30MPa.

285 **Table 9 Table of Mechanical Parameters of Rock**

Young's modulus (Gpa)	Poisson's ratio	Uniaxial compressive	Severity (KN/m ³)	The permeability	Hoek-Brown m parameter	Hoek-Brown S parameter	Fluid compressibility 1/Pa	Density kg/m ³
-----------------------	-----------------	----------------------	-------------------------------	------------------	------------------------	------------------------	----------------------------	---------------------------



strength
(MPa)

coefficient
is 10⁻⁶
cm/s.

35	0.33	122	27	2.2	2.5	0.08	4.6×10 ⁻¹⁰	103
----	------	-----	----	-----	-----	------	-----------------------	-----

The initial stress-seepage coupling is carried out by numerical simulation, and the pore water pressure field is analyzed. When the initial stress field and seepage field are coupled, the pore water pressure near the two sides of the cave is larger than that above, with the pore water pressure on the left side being about 38MPa, the pore water pressure on the right side being about 33MPa and the pore water pressure above the cave being 16MPa; At the same time, the left side is close to the karst cave, and the area with high pore water pressure is mainly concentrated around the karst cave, while the pore water pressure near the karst cave on the right side is dispersed; On the left side, the pore water pressure will gradually decrease with the increase of the distance from the left side of the cave, and finally the pore water pressure will be 0 ~ 5 MPa. After excavation, the stress and water pressure are coupled again, and finally converge. The pore water pressure on both sides of the cave is greater than that on the top, but the difference is small. The pore water pressure on the left side is about 20Mpa, the pore water pressure on the right side is about 17MPa, and the pore water pressure on the top of the cave is 13MPa;On the left side near the cave, the pore water pressure is concentrated, and on the right side near the cave, the pore water pressure is dispersed;Compared with the initial stress-seepage coupling, the pore water pressure around the initial coupled karst cave is obviously higher than that around the secondary coupled karst cave, and the maximum pore water pressure on the left side of the karst cave is greater than that on the right side of the karst cave. This is mainly because there is a tunnel on the left side of the karst cave in the initial coupling state and the secondary coupling state. The excavation of the tunnel leads to the reduction of the safe thickness of the rock layer between the left side and the tunnel, and some water inrush channels are formed, which makes the karst cave water flow into the tunnel along the water inrush channels, while the pore water pressure dispersion on the right side of the karst cave is mainly due to the fact that there is no water inrush channel on the right side, and the karst cave has no water inrush, and the water basically accumulates in the karst cave. At the same time, the pore water pressure in the secondary coupling state is smaller than that in the initial coupling state, mainly because



310 under the stress-seepage coupling, the tunnel and the karst cave form a water inrush channel, and the
karst cave water is gradually pouring into the tunnel, so the pore water pressure around the karst cave in
the secondary coupling state is smaller than that in the initial coupling state.

4 Conclusion

Water inrush disaster is the main geological disaster of water-rich and deep-buried karst tunnel, which
315 is extremely harmful and threatens tunnel construction and construction safety. This paper takes
Nahecun water-rich deep-buried karst tunnel of Tian'e through Fengshan to Bama Expressway as the
research object, analyzes the hydrogeological characteristics of karst area through geological
investigation, grasps the characteristics of groundwater occurrence and migration, finds out the main
disaster-causing factors and influencing factors of water inrush disaster in karst tunnel, reasonably
320 selects the influencing factors of water inrush and their weights to construct a combined weighting -
TOPSIS method tunnel water inrush risk assessment system, verifies the evaluation system through
field excavation experiments, and analyzes the water inrush mechanism of karst tunnel by using finite
element analysis software, which provides the water inrush risk assessment and water inrush
mechanism research for water-rich deep-buried karst tunnel. Main research results:

325 (1) Nahecun Tunnel is one of the most important tunnel projects on the Tian'e through Fengshan to
Bama Expressway, which passes through One back diagonal pleated strap, Six groups of jointed
fractures and an underground river. During the construction process, many caves are dissolved and
many water inrush accidents occur. The main influencing factors of water inrush in karst tunnel include
stratum, geological structure, landform, hydrogeological conditions and other factors, among which
330 stratum factors are mainly lithology and rock occurrence, geological structure is mainly faults and folds,
landform is mainly negative topographic area and topographic slope, hydrogeological factors mainly
consider the difference between groundwater level and tunnel elevation and karst cave water pressure,
and other factors mainly consider geostress and karst cave diameter; The analytic hierarchy process
(AHP) and entropy weight method are used to get the evaluation weight of each index. According to the
335 combined weight -TOPSIS method, the distance and relative proximity between the typical tunnel
section and the ideal solution of Nahecun tunnel are obtained, and the water inrush risk evaluation of
Nahecun tunnel section is obtained.



(2) The tunnel section with risk grade II K7+750 ~ K7+950 is selected, and the equivalent continuum model and Hoek-Brown yield criterion are adopted to establish the three-dimensional simulation model of Nahecun tunnel; Through numerical simulation, the pore water pressure is analyzed by initial stress-seepage coupling and secondary stress-seepage coupling after excavation. It is concluded that when the initial stress field and seepage field are coupled, the pore water pressure near the two sides of the cave is higher than that above, and the area near the cave on the left is concentrated around the cave, and the pore water pressure on the right side is dispersed, which will gradually decrease with the increase of the distance from the left side of the cave. After excavation, the pore water pressure on both sides near the cave is higher than that on the top, but the difference is small. The pore water pressure is concentrated on the left side near the cave and dispersed on the right side near the cave. The pore water pressure around the initial coupling cave is obviously higher than that around the secondary coupling cave, and the maximum pore water pressure on the left side of the cave is greater than that on the right side of the cave, mainly because there is a tunnel on the left side of the cave, and some water inrush channels are formed between the left side and the tunnel due to the excavation of the tunnel.

Data availability

The figures and tables used to support the findings of this study are included in the article.

Author contributions

Xin Zhang , Xiaozhen Jiang and Mingtang Lei wrote the main manuscript text. Shaoqing Wang, Xiaotian Zhang and Hai Chen performed the data analysis. Xin Zhang and Xiaozhen Jiang conducting a research and investigation process. All authors reviewed the manuscript.

Competing interests

The authors declare that they have no conflicts of interest.

Acknowledgements

The authors would like to show sincere thanks to those techniques who have contributed to this research.

Financial support

This work was supported by The Formation of Water and Air Pressure Pulsation in Karst Cavities and Its Mechanism of Triggering Sinkhole (42077273); and Mechanism and early warning of cover collapse



365 sinkhole of Guangxi red clay induced by damage under coupling effect of seepage and stress
(2023GXNSFAA026432).

References

Dai, C., Long, Y., Lv, Y., Hou, W., & Sui, H. .Water inrush mechanism and safety control in drilling and
370 blasting construction of subsea tunnel. *Journal of Coastal Research*, 94(SI), 218-
222,https://doi.org/10.2112/SI94-046.1,2019.

Dong, L., Wang, H., Song, D., Chen, J., & Liu, C. . Analysis of the catastrophe mechanism and
treatment countermeasures of a sudden water inrush disaster in a long and deeply buried tunnel in the
karst area. *Journal of Performance of Constructed Facilities*, 37(6),
375 06023002,https://doi.org/10.1016/j.engfailanal.2023.

Fu, H., An, P., Cheng, G., Li, J., Huang, Z., & Yu, X. Calculation of the safety thickness of water inrush
with tunnel axis orthogonal to fault. *Arabian Journal of Geosciences*, 14, 1-
11,https://doi.org/10.1007/s12517-021-07297-8,2021.

Han, G., Xue, P., Wang, Y., Li, X., Bian, H., Wang, Y., & Guo, P. Mechanical Response Law and
380 Parameter Influence Analysis of Karst Tunnel Dynamic Excavation. *Applied Sciences*, 13(16),
9351, https://doi.org/10.3390/app13169351,2023.

He, Y., Wang, H., Zhou, J., Su, H., Luo, L., & Zhang, B. Water Inrush Mechanism and Treatment
Measures in Huali Highway Banyanzi Tunnel—A Case Study. *Water*, 15(3),
551,https://doi.org/10.3390/w15030551,2023.

385 Huang, M., Li, J., Yang, Z., Zhang, Z., & Song, Y. Analysis and application of lining resistance to water
pressure in tunnel through karst cave. *Applied Sciences*, 12(15),
7605,https://doi.org/10.3390/app12157605,2022.

Jana, C., Muhiuddin, G., Pal, M., & Al-Kadi, D. . Intuitionistic fuzzy dombi hybrid decision-making
method and their applications to enterprise financial performance evaluation. *Mathematical Problems in*
390 *Engineering*, 2021, 1-14, https://doi.org/10.1155/2021/3218133,2021



- Jiang, X., Lei, M. & Zhao, H. Review of the advanced monitoring technology of groundwater–air pressure (enclosed potentiometric) for karst collapse studies. *Environ Earth Sci* 78, 701. <https://doi.org/10.1007/s12665-019-8716-z>,2019.
- Jiang, Y., Zhou, P., Zhou, F., Lin, J., Li, J., Lin, M., ... & Wang, Z. . Failure analysis and control
395 measures for tunnel faces in water-rich sandy dolomite formations. *Engineering Failure Analysis*, 138, 106350,<https://doi.org/10.1016/j.engfailanal.,2022>.
- Li, D., Xu, H., Jiang, T., Ding, H., & Xiang, Y. . Tunnel water burst disaster management engineering based on artificial intelligence technology–taking Yonglian Tunnel in Jiangxi Province as the object in China. *Water Supply*, 23(8), 3377-3391,<https://doi.org/10.2166/ws.2023.170>,2023
- 400 Li, K., Li, H., & Liu, Z. .Appraisal of a galvanic-source transient electromagnetic method for hazardous water structures beyond tunnel sidewall. *Environmental Earth Sciences*, 82(21), 520,<https://doi.org/10.1007/s12665-023-11208-3>,2023.
- Liu, B., Ye, W., Zhu, C., Chen, R., Huang, S., & Ni, X. Analysis on treatment effect of mine tunnel construction spring in karst area. *Mathematical Problems in Engineering*, 1-
405 11, <https://doi.org/10.1155/2021/5585054>,2021.
- Liu, W., Yang, X., Gao, X., Zeng, S., Zhou, J., Wu, X., & Zhang, J. Impacts of water surge from mountain railroad tunnels on ecological environments based on the RSEI model. *Environmental Science and Pollution Research*, 30(57), 120400-12042,<https://doi.org/10.1007/s11356-023-30728-w>,2023
- Liu, Y., Feng, Y., Xu, M. et al. Effect of an incremental change in external water pressure on tunnel
410 lining: a case study from the Tongxi karst tunnel. *Nat Hazards* 98, 343–377, <https://doi.org/10.1007/s11069-019-03692-3>,2019
- Luo, X., Yu, C., & Wang, Y. Water control of water-rich deeply buried tunnel: an analytical model of a combined scheme. *Geotechnical and Geological Engineering*, 41(7), 3909-3922,<https://doi.org/10.1007/s10706-023-02495-5>,2023.
- 415 Shan Wu, Weichao Qiu, Dunwen Liu, Yu Tang, "Grouting Treatment and Parameters Optimization in Watery Karst Areas of High Speed Railway Tunnel Based on Comprehensive Geological Forecast: A Case Study", *Geofluids*, vol.,Article ID 7582916, 23 ,<https://doi.org/10.1155/2022/7582916>,2022.



- Su, C., Hu, Q., Yang, Z., & Huo, R. A Review of Deep Learning Applications in Tunneling and Underground Engineering in China. *Applied Sciences*, 14(5),
420 1720.<https://doi.org/10.3390/app14051720,2024>
- Sun, X., Teng, G., Guo, X., & Li, X..Risk assessment of water inrush in karst tunnels based on fuzzy comprehensive evaluation considering misjudgment losses: a case study. *Arabian journal of geosciences*, 15(5), 421,<https://doi.org/10.1007/s12517-022-09633-y,2022>.
- Tang, Y., Zhang, Q., Qi, J., Xu, M., Li, X., Qu, C., & Wang, D. (2023). Change analysis of karst
425 landforms, hydrogeological conditions and effects of tunnel excavation on groundwater environment in three topography grades in China. *Water*, 15(1),207,<https://doi.org/10.3390/w15010207,2023>.
- Wang, S., Li, L., Cheng, S. et al. Model on Improved Variable Weight-Matter Element Theory for Risk Assessment of Water Inrush in Karst Tunnels. *Geotech Geol Eng*, 39,3533–3548.,
<https://doi.org/10.1007/s10706-021-01709-y,2021>
- 430 Wang, X., Shi, K., Shi, Q., Dong, H., & Chen, M. . A normal cloud model-based method for risk assessment of water inrush and its application in a super-long tunnel constructed by a tunnel boring machine in the arid area of northwest China. *Water*, 12(3), 644,<https://doi.org/10.3390/w12030644,2020>
- Xiao, Q., Li, S., Ye, F., Qian, R., Liao, H., Ye, B., & Fu, W. Explicit analytical solution to the minimum safety thickness of waterproof-resistant slab in front of karst tunnel face. *Engineering Failure*
435 *Analysis*, 157, 107941.<https://doi.org/10.1016/j.engfailanal.2023.107941,2024>
- Yang, W., Fang, Z., Wang, H., Li, L., Shi, S., Ding, R., ... & Wang, M. Analysis on water inrush process of tunnel with large buried depth and high water pressure. *Processes*, 7(3),
134.<https://doi.org/10.3390/pr7030134,2019>
- Zhang, J., Li, S., Zhang, Q., Zhang, X., Li, P., Wang, D., & Weng, X. Mud inrush flow mechanisms: a
440 case study in a water-rich fault tunnel. *Bulletin of Engineering Geology and the Environment*, 78, 6267-6283,<https://doi.org/10.1007/s10064-019-01508-z,2019>
- Zhang, N., Niu, M., Wan, F., Lu, J., Wang, Y., Yan, X., & Zhou, C.Hazard Prediction of Water Inrush in Water-Rich Tunnels Based on Random Forest Algorithm. *Applied Sciences*, 14(2),
867,<https://doi.org/10.3390/app14020867,2024>



- 445 Zhang, W., Zhou, X., Wei, W., & Cheng, X. Risk assessment of water inrush in tunnels: a case study of a tunnel in Guangdong province, China. *Sustainability*, 14(18), 11443, <https://doi.org/10.3390/su141811443>, 2022.